View metadata, citation and similar papers at core.ac.uk
brought to you by CORE
provided by Open Archive Toulouse Archive Ouverte

Development of an original model for the synthesis of silicon nanodots by Low Pressure Chemical Vapor Deposition

V. Cocheteau [a,b], P. Mur [b], T. Billon [b], E. Scheid [c], B. Caussat [a,*]

[a] LGC/ENSIACET/INPT, UMR CNRS 5503, 5 rue Paulin Talabot, BP1301, 31106 Toulouse Cedex 1, France
[b] CEA-DRT-LETI – CEA-GRE, 17 Avenue des Martyrs, 38054 Grenoble Cedex 09, France
[c] LAAS, UPR CNRS 8011, Avenue du Colonel Roche, 31077 Toulouse Cedex, France

Keywords:
CVD
Electronic materials
Silicon nanodots
CFD
Kinetics
Multiphase reactions

A B S T R A C T

Using the Computational Fluid Dynamics code Fluent, a simulation model of an industrial Low Pressure Chemical Vapor Deposition reactor has been developed for the synthesis of silicon nanodots from silane SiH_4 on silicon dioxide SiO_2 substrates. A comparison between experimental and simulated deposition rates has shown that classical kinetic laws largely over-estimated these deposits. So, an original heterogeneous kinetic model is proposed as a first attempt to quantify the temporal evolution of deposition rates and of surface site numbers, as a function of operating conditions and of the chemical nature of substrate sites, for the early stages of silicon deposition. Contributions of silane and of the homogeneously born silylene SiH_2 to nucleation and growth have been considered on different surface sites, silanol Si–OH, siloxane Si–O–Si and fresh silicon bonds. Simulations have revealed that for the conditions tested, the classical heterogeneous kinetic laws over-estimate, by more than 60%, silicon deposition during the first stages. The assumption that silylene and more largely all the unsaturated species formed in the gas phase contribute in priority to nucleation has been validated. Nucleation appears as a mandatory step to form the first fresh Si sites to allow deposition to occur from silane via growth phenomena.

1. Introduction

Understanding the phenomena involved in the initial stages of silicon film formation by Low Pressure Chemical Vapor Deposition (LPCVD) from silane SiH_4 is becoming increasingly important. This is due to the never-ending demand for higher integration in microelectronics, and to the unique physical properties of silicon nanodots (NDs) spontaneously formed on oxidised silicon during this stage [1–2]. Indeed the development of novel devices such as non-volatile memories (NVM) and single electron transistors (SET) has become possible thanks to size confinement effects and Coulomb blockade phenomena observed for ND structures [3–5].

These physical properties are strongly dependent on the ND size distribution, area density and shape [4,6–7]. Area densities of 10^{12} NDs/cm^2 corresponding to NDs of 5 nm in diameter spaced 5 nm apart are sought for optimal device performance [7,8]. As a consequence, it is mandatory to have a thorough understanding of the phenomena involved in the nucleation, growth and coalescence of NDs.

* Corresponding author at: Laboratoire de Génie Chimique, ENSIACET/Institut National Polytechnique de Toulouse, 5 rue Paulin Talabot, BP1301, 31106 Toulouse Cedex 1, France. Tel.: +33 5 34 61 52 11; fax: +33 5 34 61 52 53.
E-mail address: Brigitte.Caussat@ensiacet.fr (B. Caussat).

While a general comprehension of silicon ND nucleation and growth exists, a more accurate model is still required to optimize the synthesis conditions to adapt the process to industry. According to Leach et al. [9], mobile silicon adatoms are present during the deposition of silicon atoms on dielectric surfaces such as SiO_2. These adatoms are thought to accumulate and cluster to form stable nuclei that grow to cover the surface and eventually coalesce [10]. This model provides a simple picture of the surface mechanisms. Nevertheless, questions remain about the influence of the main operating parameters and the effect of substrate pre-treatments, which modify the surface reactivity.

The outer surface of thermal silicon dioxide substrates is composed of siloxane Si–O–Si and silanol Si–OH bonds [11]. According to these authors, at least three different silanol bonds have been identified: isolated or simple, vicinal and geminal ones. The respective proportions of each of these bonds on a given surface are difficult to measure. They depend on the exact oxidation conditions, on any surface pre-treatment received and on the thermal history of the substrate. Siloxane bonds are known to be more thermally stable and less reactive than silanol bonds [11]. Miyazaki et al. [12], Mazen [13] and Mazen et al. [7] have shown that pre-treatment of SiO_2 surfaces with hydrofluoric acid (HF) increases the area density of silanol bonds and also, proportionally, that of silicon NDs synthesized by LPCVD while the ND size decreases. The use of SiO_2 substrates with high Si–OH bond densities is then a key to reach

high NDs densities useful for quantum devices [7,11]. Mazen et al. [7] have shown, using Fourier Transform Infra-Red (FTIR) spectroscopy that the silanol bond area density of a HF treated SiO_2 substrate is close to 10^{14} cm^{-2}.

Nicotra et al. [6,8] investigated Si ND formation by energy-filtered transmission electron microscopy (EFTEM). They obtained some important results: (i) the NDs show a good wetting of the oxidised surface and their shape can be represented by a truncated sphere, (ii) a continuous steady state nucleation has been evidenced, i.e. a small limitation in the number of nucleation sites occurs during ND deposition. Puglisi et al. [14] found that on variously pre-treated SiO_2 substrates, Si NDs are always separated by a distance of at least 4 nm. They attributed this phenomenon to the existence of a capture zone within which newly deposited Si monomers preferentially contribute to growth on a previously nucleated seed, rather than aggregate to form a new nucleus. They estimated the surface diffusion coefficient of Si adatoms to be close to 10^{-15} cm^2/s at 823 K.

For Kajikawa and Noda [15], CVD processes are characterized by the existence of an incubation time, corresponding to the lag time for deposition during its initial stage. Within the incubation period, film deposition is slower than during continuous film growth, and the deposition rate grows exponentially with time. This means that the deposited material enhances deposition as in an autocatalytic process. These authors state that the large differences in the sticking probability of CVD precursors cannot only explain this incubation time, but also act on the mechanisms of ND nucleation and growth. Indeed, it is well known that for classical LPCVD conditions, silane homogeneously decomposes into unsaturated molecules Si_nH_{2n} and polysilanes Si_nH_{2n+2} [16,17]. All these species can contribute to silicon deposition. But the sticking coefficient of all unsaturated species is known to be equal to one whereas that of saturated molecules is at least several orders lower [18–20]. It is then likely that these various silicon precursors contribute differently to nucleation and growth phenomena during the first stages of Si film formation on SiO_2 substrates. Miyazaki et al. [12] measured activation energy for nucleation on HF pre-treated substrates as being half that on non-treated surfaces; they explain this fact by the reaction of the unsaturated silylene SiH_2 on silanol bonds. Mazen et al. [7] also suggest that SiH_2 could play a major role in nucleation and growth of NDs. However, these points have been little investigated and many determining elements remain unknown.

Numerous authors have developed numerical models of CVD reactors linking the elaboration conditions to the deposition rate of each of the species [18,21–23]. To our knowledge, all these works concern conventional silicon layers of thicknesses at least equal to several tens of nanometers. This is probably the reason why none of these simulation models considered the possible influence of the substrate thickness or of deposition duration.

The present work aims to adapt a numerical model, representing silicon deposition from silane in an industrial LPCVD reactor, to the simulation of ND formation on various silicon oxide substrates. The objectives are to develop a numerical tool able to predict the influence of synthesis conditions and of the nature of the substrate on ND features and more largely to progress in the understanding of the physical and chemical mechanisms involved in the first stage of Si film formation on a given substrate. An original heterogeneous kinetic model able to represent ND formation was then developed on the basis of experimental data. The synthesis and characterization features of NDs are presented first together with the main experimental results. The Computational Fluid Dynamics (CFD) software Fluent was used to model the process. The features of the model are then presented before going into details of the new heterogeneous kinetic model and the associated results.

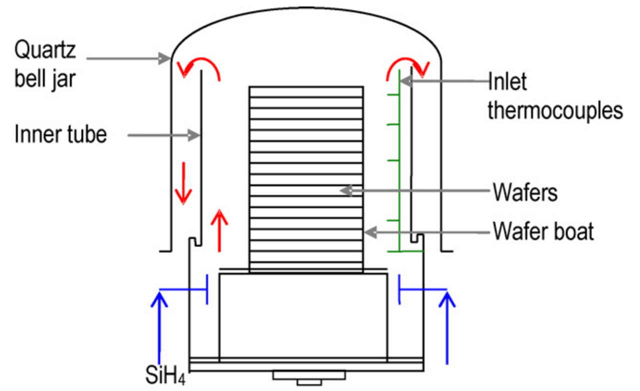

Fig. 1. Schema of the industrial LPCVD tubular reactor.

2. Experimental

2.1. Synthesis and characterization features

Silicon NDs were deposited in an industrial tubular hot wall LPCVD reactor from Tokyo Electronic Limited (TEL), as schematically presented in Fig. 1. The reactor is composed of a vertical quartz bell jar, ID 35 and 96.9 cm high, closed in its upper part by a bell 6 cm high. In the bottom of the bell jar, a 36 cm high quartz pedestal of 26.8 cm in diameter supports the wafer boat. 170 ⟨1 0 0⟩ silicon wafers 8 in. in diameter can be treated per run. They are placed horizontally, a few millimetres from each other, on the quartz boat. Gases are fed from the bottom part of the reactor; they flow upward perpendicular to the wafers in an annular region of 3.4 cm width around the boat. They are exhausted downward through the outer 4 cm wide gap between the bell jar and the central tube. Test wafers are loaded near the bottom of the boat in its first third.

The Si wafers were all thermally oxidised in dry mode at 1123 K. Two kinds of SiO_2 substrate were studied: a “non-treated” and a “treated” one. The SiO_2 thickness for the “non-treated” substrate was 5 nm. Prior to deposition, standard ozone cleaning was performed. According to Mazen [13], dry oxidation mainly provides siloxane Si–O–Si surface bonds. For the “treated” substrates, a 7 nm thick dry silicon dioxide layer was grown and just before deposition, a thickness of 2 nm was etched off in a dilute (0.2%) aqueous HF solution. The HF etching breaks the Si–O–Si bridges to form much more reactive silanol Si–OH bonds as measured by Mazen [13].

Deposition was analysed by Field Effect Gun Scanning Electron Microscopy (FEG SEM) on a Hitachi S5000 microscope, and by spectroscopic ellipsometry on a KLA Tencor UV1280. ND density was measured by direct counting on FEG SEM images. Average values were taken for three counts.

Spectroscopic ellipsometry allowed the determination of the equivalent thickness and the silicon fraction of a continuous layer including vacuum and silicon (Effective Medium Approximation model). The diameter D of the as-deposited NDs was calculated by assuming the NDs to be hemispherical and using the following equation:

$$\pi \times \frac{D^3}{12} = \frac{e_{Si}}{d_{dot}} \quad (1)$$

where e_{Si} is the equivalent thickness of silicon and d_{dot} is the ND density (in number of NDs/cm^2); the intrinsic error on ND density and radius measurements was about 7%.

2.2. Operating conditions tested and experimental results

Table 1 gives the operating conditions of the experiments retained for this study, from Cocheteau [24] and Mazen [13]. Total

Table 1
Experimental conditions tested and corresponding results

Run	Temperature (K)	P/P_{ref}	Deposition time (s)	Nature of the substrate	Nucleation rate ($\text{kmol m}^{-2}\,\text{s}^{-1}$)	Flux of deposited Si atoms ($\text{kmol m}^{-2}\,\text{s}^{-1}$)
T06	863	2	15	"Treated"	2.82×10^{-10}	2.66×10^{-9}
T07	873	2	7	"Treated"		7.12×10^{-9}
T31	873	3.375	5	"Non-treated"	4.314×10^{-10}	2.303×10^{-9}
T32	873	3.375	10	"Non-treated"		3.189×10^{-9}
T33	873	3.375	15	"Non-treated"		1.072×10^{-8}
T39	873	1	30	"Non-treated"	1.506×10^{-10}	2.852×10^{-9}
T40	873	1	40	"Non-treated"		2.657×10^{-9}

P is the total pressure of work and P_{ref} corresponds to a total pressure of reference.

pressures were fixed between 5 and 40 Pa. Only a few runs among the many performed could be considered here because for the conditions tested, coalescence occurred very frequently, especially on "treated" substrates. Only runs leading to non-coalesced NDs were retained, even though coalescence was close for runs T39–T40.

The corresponding experimental ND densities and radii are given in Fig. 2. Densities were between 2×10^{11} and 8×10^{11} NDs/cm^2. They were of course higher on "treated" substrates. ND radii varied between 2 and 5 nm and were the lowest for the "treated" substrates. It can be observed that both densities and radii tended to increase with time, till the beginning of coalescence, at which densities became constant and then decreased. By comparing runs T39–T40 and T31–T32–T33, ND densities increased with the total pressure. The influence of temperature cannot be inferred from these data (since it has been maintained close to 873 K), but Mazen et al. [3] have shown that temperature has a lower influence than pressure on ND features. Note that despite numerous TEM (Transmission Electron Microscopy) analyses, the exact crystalline nature of the NDs could not be determined due to their nanometric size [25]. But all high resolution TEM of NDs deposited between 570 and 650 °C, show that NDs are crystalline [26]. This range of temperature was that of our whole runs.

3. CFD model general features

Phenomena involved in the LPCVD process include tightly coupled fluid flow, heat transfer, mass transport of multiple gas species and chemical reactions in the gas phase and on surfaces of the reactive zone. As a consequence, a numerical model for this process involves partial differential equations describing the conservation of mass, momentum, energy and chemical species, associated to appropriate boundary conditions.

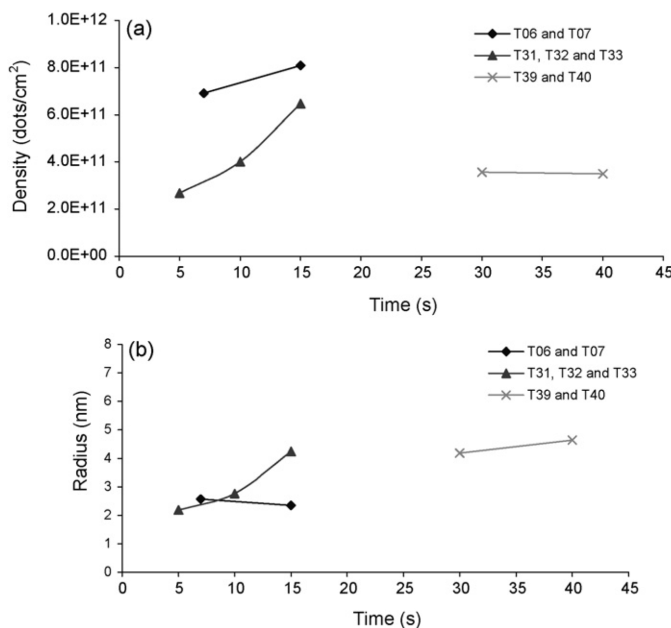

Fig. 2. Experimental ND (a) densities and (b) radii versus deposition time.

The reactor has been simulated using the commercial CFD software Fluent [27]. Fluent is a pressure-based, implicit Reynolds Averaged Navier Stokes solver that employs a cell-centered finite volume scheme having second-order spatial accuracy. This software discretizes any computational domain into elemental control volumes, and permits the use of quadrilateral or hexahedral, triangular or tetrahedral and hybrid meshes.

Gas flow, heat and mass transfers including homogeneous and heterogeneous chemical reactions were calculated.

The following assumptions were made:

- gas flow is laminar (*Re* number lower than 30),
- the gas is ideal,
- due to its small surface area compared to the total silicon wafer area, the presence of the quartz wafer boat is ignored,
- the reactive zone is considered as axially symmetric so only a plane corresponding to a radius of the reactor has been studied,
- compressibility effects have not been considered since the Mach number is at maximum equal to 0.012,
- heats of reaction are ignored,
- the reactive zone and the gas phase are assumed to be isothermal, the temperature being fixed at the experimental one,
- simulations are performed in transient conditions, to account for the temporal evolution of the surface sites and of the reactivity of the precursors.

A 2D geometrical domain of 25,000 non-structured meshes is used to represent the whole reactive zone. The associated boundary conditions are the following:

- at the gas inlet, a flat profile is imposed on gas velocity; the total mass flux of species is fixed to the experimental one,
- at the symmetry axis and at the exit, classical Danckwerts conditions (diffusive flux densities equal to zero), are applied for gas velocity and mass fractions,
- on the walls and wafer surfaces, a classical no-slip condition is used for gas velocity; the mass flux density of each species is assumed to be equal to the corresponding heterogeneous reaction rate,
- at the exit, the total pressure is fixed at the experimental value.

The physical properties of the gaseous mixture were calculated from the Fluent data base. The time step was fixed at 10^{-3} s.

The classical homogeneous chemical reactions considered and the corresponding kinetic constants are listed in Table 2 from Fayolle et al. [28] and Cordier et al. [20]. By considering only silane SiH_4 and silylene SiH_2 as silicon precursors, the kinetic scheme was wit-

Table 2
Chemical reactions and kinetic laws retained

Chemical reaction	Kinetic law
$SiH_4 \leftrightarrow SiH_2 + H_2$	Kinetic constant of the silane decomposition reaction (s^{-1}) $7.1 \times 10^7 \times P \times \exp(-197.1 \times 10^3/(RT))$ Kinetic constant of the silane formation reaction ($m^3\ mol^{-1}\ s^{-1}$) $2 \times 10^2 \times P \times \exp(900 \times 10^3/(RT))$
$SiH_4 \rightarrow Si + 2H_2$	$R_{SiH_4} = \frac{kP_{SiH_4}}{1+k_1 P_{H_4} + k_2 P_{SiH_4}}$ (in $kmol\ m^{-2}\ s^{-1}$) with $k = 3.2 \times 10^{-6} \exp\left(\frac{-6800}{T}\right)$ (in $kmol\ m^{-2}\ s^{-1}\ Pa^{-1}$) $k_1 = 4.8 \times 10^{-8} \exp\left(\frac{10000}{T}\right)$ (in Pa^{-1}) $k_2 = 8.2 \times 10^{-10} \exp\left(\frac{18000}{T}\right)$ (in Pa^{-1})
$SiH_2 \rightarrow Si + H_2$	$R_{SiH_2} = \gamma_{SiH_2} \times \frac{1}{4}\sqrt{\frac{8RT}{\pi M_{SiH_2}}} \times \frac{1}{RT} \times y_{SiH_2} \times P$ (in $kmol\ m^{-2}\ s^{-1}$) with γ_{SiH_2} the sticking coefficient of SiH_2 equal to 1, y_{SiH_2} its molar fraction, M_{SiH_2} its molar weight, and P the total pressure

tingly simplified to reduce the duration of calculation. However, this choice does not limit the interest of the model because silylene SiH_2 is the main unsaturated species created in the gas phase and secondly it is well known that the contribution to the deposits of polysilanes of order higher than 2 is negligible in LPCVD conditions [18,20].

The associated heterogeneous reactions are also detailed in Table 2, with their kinetic laws. For silane, the overall empirical law of Wilke et al. [29] was retained, valid for total pressures lower than 133 Pa. It is well known that due their extremely high reactivity, all the unsaturated species chemisorb instantaneously whatever the surface site [18,20]. Consequently, for silylene SiH_2, a sticking coefficient equal to one was classically assumed, and the kinetic theory of gases was used to calculate the deposition rate.

As reported elsewhere [24,25], numerous experiments performed in the TEL LPCVD reactor have been simulated with the conventional kinetic laws described above. A comparison of the experimental and calculated deposition rates is given in Fig. 3 for non-treated and treated substrates, and for the bottom, middle and top parts of the wafers load. A perfect agreement would correspond to points on the diagonal.

All the calculated values are much higher than the experimental ones. Most often, the discrepancy is higher for the bottom part of load near the silane entrance, because the deposition rates calculated by Fluent decrease from the bottom to the top parts of the reactor, whereas the experimental values are in general more uniform. Moreover, Fig. 3(b) shows that the discrepancy is lower for treated substrates, since the experimental NDs deposition rates are higher on treated wafers thanks to the higher substrate reactivity.

To explain why the calculated values are much higher than the experimental ones, it is to be known that the empirical heterogeneous kinetic law of Wilke et al. [29] was established for thick Si layers (of at least several tens of nanometers), for which the influence of the substrate is limited. The situation is drastically different for NDs: the nature of the substrate is of major importance and it is likely that a SiO_2 surface, even mainly composed of silanol bonds, has a lower reactivity toward a saturated molecule like silane, than a fresh Si layer presenting numerous dangling bonds. From our point of view, unsaturated molecules like SiH_2 are clearly much less sensitive to the substrate nature thanks to their extremely high reactivity.

So, a new heterogeneous kinetic model was developed, based on the main assumption that the kinetic law of Wilke et al. [29] only predicts silane physisorption, not chemisorption, thus allowing the possibility for physisorbed silane molecules to desorb, as detailed below.

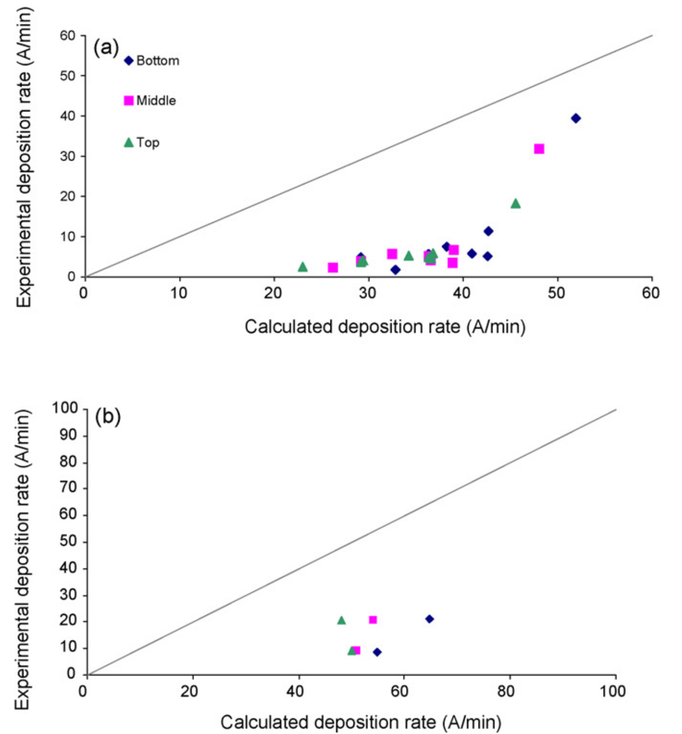

Fig. 3. Comparison of experimental and calculated deposition rates using the original kinetic law of Wilke et al. [29] for runs performed on (a) non-treated substrates and (b) treated wafers.

4. Principles and assumptions of the new heterogeneous kinetic model

4.1. Substrate surface features

As already explained in Section 2, two kinds of SiO_2 substrates have been investigated, the "non-treated" one, mainly presenting siloxane Si–O–Si surface bridges, and the "treated" one mainly composed of silanol Si–OH surface bonds. As explained in the introduction, silanol bonds are heat-sensitive and tend to form siloxane bridges above 873 K [11]. The quantification of the ratio of the various surface bonds of SiO_2 substrates heated around 873 K before and during deposits is then extremely difficult to perform.

The first assumption of this work is then to consider that a "non-treated" substrate exclusively presents a Si–O–Si siloxane ter-

minated surface whereas a “treated” substrate only presents simple Si–OH silanol surface bonds.

As a consequence, two kinds of deposition sites can coexist during deposition: (i) siloxane or simple silanol bonds and (ii) fresh Si dangling bonds corresponding to silicon atoms just chemisorbed.

We saw in the introduction that according to Mazen et al. measurements by FTIR spectroscopy [7], a “treated” substrate roughly presents 10^{14} silanol bonds/cm^2 just after HF etching. In order to obtain a more precise value, we calculated the atom number existing on a β-crystobalite SiO_2 surface which is a classical SiO_2 structure [30]. On this cubic face-centered structure whose mesh size is 0.716 nm, a density of 3.9×10^{14} surface bonds/cm^2 was found, quite close to Mazen's value [7].

It is important to note that these values are probably under-estimated because we have seen in Section 2.2 that for the conditions tested, the maximum ND density obtained is 8×10^{11} cm^{-2}. Fig. 2 shows that NDs have a mean radius close to 3 nm; this roughly leads to 500 Si atoms/ND present at the SiO_2/Si interface by assuming that NDs are hemispherical and a diamond fcc arrangement of their Si atoms. This should correspond to about 4×10^{14} OH/Si bonds/cm^2, which would mean that all the surface bonds are active for nucleation, which is not the case [14]. Without any possibility to obtain more precise values for the initial SiO_2 surface bonds, we supposed for the present work that all our substrates present 3.9×10^{14} surface bonds/cm^2.

We also assumed that the total number of deposition sites is constant and remains equal to this value during deposition. This means that each surface site only allows the chemisorption of one Si atom, which seems quite reasonable.

4.2. Physical and chemical phenomena considered

In the new model, we have assumed that the law of Wilke et al. [29] exclusively predicts a number of physisorbed molecules. In a subsequent step, these ad-species can:

- either chemisorb directly on their physisorption site,
- or chemisorb on a fresh Si site after surface diffusion,
- or desorb without reacting.

This scheme only concerns silane SiH_4. For silylene SiH_2, we still assume that it chemisorbs instantaneously on its physisorption site.

Moreover, in our representation, nucleation corresponds to silicon chemisorption exclusively on a substrate site, i.e. on a Si–OH or Si–O–Si bond, whereas growth stands for Si chemisorption only on a fresh Si site. This representation does not exactly reflect real phenomena since nucleation generally corresponds to the first chemisorbed atoms around which new atoms deposit laterally as well as vertically thus contributing to growth. Our vision tends to over-estimate nucleation to the detriment of growth *stricto sensu*.

Then, because of the unsaturated nature of SiH_2, we assumed that it contributes in priority to nucleation on Si–O–Si as on Si–OH bonds. If this contribution is not sufficient to account for the experimental nucleation, i.e. if the deposition rate of SiH_2 on these surface sites is lower than the experimental nucleation rate, the difference is filled in by silane contribution.

In contrast, if the SiH_2 deposition rate on these Si–O–Si or Si–OH bonds exceeds the experimental nucleation rate, only SiH_2 contributes to nucleation and this species could desorb or chemisorb after surface diffusion. But this would be in contradiction with the present work. Fortunately, this case never occurred for any of the conditions tested.

The remaining silane which has not participated in nucleation but which has physisorbed can then either diffuse on surface and chemisorb on a fresh Si bond, thus contributing to growth, or desorb. The exact calculation of the silane fluxes concerned by these two latter phenomena is performed by mass balance from experimental data, as explained below.

From a mechanistic point of view, the present model considers (i) a continuous nucleation all along ND synthesis, as found by Nicotra et al. [6], (ii) a possible surface diffusion of silicon adatoms before chemisorption on a fresh Si site (i.e. growth), as thought in particular by Puglisi et al. [14], (iii) an autocatalytic role of the already deposited silicon atoms, as proposed by Kajikawa and Noda [15] and (iv) a specific role for SiH_2 regarding nucleation as mentioned by Miyazaki et al. [12].

4.3. New formulation of the heterogeneous kinetic laws

For the two gaseous precursors SiH_4 and SiH_2, the laws were balanced by kind of site and by considering the proportion of silane

Table 3
New formulation of the heterogeneous kinetic laws

Event	New form of kinetic law
Deposition rate from SiH_4	
Nucleation on a Si–OH or Si–O–Si site	$R_{SiH_4/SiOSi\ nucleation} = \frac{K_1 P_{SiH_4}}{1+K_H P_{H_2}+K_S P_{SiH_4}} \times \frac{n_{site\ SiOSi}}{n_{site\ total}} \times x_{nucleation\ SiOSi}$
	$R_{SiH_4/SiOH\ nucleation} = \frac{K_1 P_{SiH_4}}{1+K_H P_{H_2}+K_S P_{SiH_4}} \times \frac{n_{site\ SiOH}}{n_{site\ total}} \times x_{nucleation\ SiOH}$
Physisorption on a Si–OH or Si–O–Si site then surface diffusion and chemisorption on a fresh Si site	$R_{SiH_4/SiOSi\ diffusion} = \frac{K_1 P_{SiH_4}}{1+K_H P_{H_2}+K_S P_{SiH_4}} \times \frac{n_{site\ SiOSi}}{n_{site\ total}} \times x_{diffusion\ SiOSi}$
	$R_{SiH_4/SiOH\ diffusion} = \frac{K_1 P_{SiH_4}}{1+K_H P_{H_2}+K_S P_{SiH_4}} \times \frac{n_{site\ SiOH}}{n_{site\ total}} \times x_{diffusion\ SiOH}$
Growth on a fresh Si site	$R_{SiH_4/Si} = \frac{K_1 P_{SiH_4}}{1+K_H P_{H_2}+K_S P_{SiH_4}} \times \frac{n_{site\ Si}}{n_{site\ total}}$
Desorption rate from SiH_4	
Physisorption on a Si–OH or Si–O–Si site then desorption	$R_{SiH_4/SiOSi\ desorption} = \frac{K_1 P_{SiH_4}}{1+K_H P_{H_2}+K_S P_{SiH_4}} \times \frac{n_{site\ SiOSi}}{n_{site\ total}} \times x_{desorption\ SiOSi}$
	$R_{SiH_4/SiOH\ desorption} = \frac{K_1 P_{SiH_4}}{1+K_H P_{H_2}+K_S P_{SiH_4}} \times \frac{n_{site\ SiOH}}{n_{site\ total}} \times x_{desorption\ SiOH}$
Deposition rate from SiH_2	
Nucleation on a Si–OH or Si–O–Si site	$R_{SiH_2/SiOH} = \sqrt{\frac{1}{2\pi M_{SiH_2} RT}} \times \frac{n_{site\ SiOH}}{n_{site\ total}}$
	$R_{SiH_2/SiOSi} = \sqrt{\frac{1}{2\pi M_{SiH_2} RT}} \times \frac{n_{site\ SiOSi}}{n_{site\ total}}$
Growth on a fresh Si site	$R_{SiH_2/Si} = \sqrt{\frac{1}{2\pi M_{SiH_2} RT}} \times \frac{n_{site\ Si}}{n_{site\ total}}$

The x_k terms appearing in the table are related to the y_k ones by: $x_k = y_k \times (R_{SiH_4/Si} + R_{SiH_4/SiOH\ or\ SiOSi})/R_{SiH_4/SiOH\ or\ SiOSi})$.

or silylene physisorbing either on a substrate bond or on a fresh Si one. Moreover, for the proportion of silane physisorbed on a Si–O–Si or Si–OH site, the kinetic law has also been balanced to account for desorption. These new formulations are given in Table 3.

The fractions of Si atoms from silane contributing to nucleation, surface diffusion/chemisorption and desorption have respectively been calculated from the following expressions:

$$y_\text{nucleation} = \frac{(V_\text{nucl} - R_{\text{SiH}_2/\text{SiOH or SiOSi}})}{(R_{\text{SiH}_4/\text{Si}} + R_{\text{SiH}_4/\text{SiOH or SiOSi}})} \quad (2)$$

$$y_\text{desorption} = \frac{(R_{\text{SiH}_4/\text{Si}} + R_{\text{SiH}_4/\text{SiOH}} - V_\text{exp})}{(R_{\text{SiH}_4/\text{Si}} + R_{\text{SiH}_4/\text{SiOH or SiOSi}})} \quad (3)$$

$$y_\text{diffusion} = 1 - y_\text{nucleation} - y_\text{desorption} \quad (4)$$

where $R_{i/j}$ is the calculated silicon deposition rate (in kmol m^{-2} s^{-1}) from the gaseous species *i* on the surface site *j*.

The various events considered in the new model were thus quantified from experimental values of the nucleation rate V_nucl and of the total flux of Si atoms deposited V_exp, calculated as follows. As detailed in Section 2, for a given set of operating conditions, the mean area density and diameter of NDs are known for a given deposition duration or sometimes for different durations. From this experimental information, the methodology of calculation is based on the following assumptions:

- NDs are hemispherical, as found by Nicotra et al. [6,8],
- all NDs have the same radius, equal to the mean radius calculated from relation (1). This radius corresponds to the base of the full hemisphere,
- as explained in Section 2, it is difficult to know the crystal nature of the NDs, and hence the crystal mesh parameters. In a first approach, we therefore assumed a diamond arrangement of the ND Si atoms and we considered the (1 0 0) face.

Note that as the NDs are considered as hemispherical, the validity of the model is limited to non-coalesced layers, i.e. those for which NDs can undoubtedly be considered as hemispherical.

The nucleation rate was calculated by combining the experimental density and size. First, the number of Si atoms at the base of the NDs can be easily calculated knowing the radius of a Si atom (0.115 nm), and the mean radius of NDs. It is interesting to note that this mean number of Si atoms was comprised between 280 and 1100 for the conditions tested. The nucleation rate (expressed in Si atom number/cm^2 s) is equal to the slope of the curve corresponding to the density in Si atoms/cm^2 versus time. However, especially for runs T39–T40, the temporal evolution of this rate was poorly physical. This is due to the intrinsic measurement errors and to the fact that coalescence was very close. In these conditions, in a first approach, a constant mean value was considered for all the nucleation rates, as given in Table 1. In the simulations all performed in transient mode, this constant value is replaced by a nil value at the time corresponding to the presumed beginning of coalescence; the various chemisorbed species then contribute exclusively to growth. The resulting nucleation rates are given in Table 1.

It can be observed that a temperature increase at a fixed pressure leads to an increase of the mean nucleation rate, as does an increase of pressure at a fixed temperature. This rate is logically higher for the “treated” substrates than for the “non-treated” ones.

The total number of Si atoms deposited/cm^2 has been estimated by multiplying the ND area density expressed in NDs/cm^2 by the number of atoms present in a dot. The resulting values are also given in Table 1. As expected, the total number of atoms deposited tends to increase with deposition duration. However, some artefacts also appeared as can be seen in Table 1. The intrinsic errors on the measurements were also the cause. In a first approach, we decided to consider in our study an increasing number of Si atoms deposited with run duration on the basis of these values.

It is worth noting that the model presented here uses the nucleation rate and the flux of deposited atoms (proportional to the deposition rate) as input parameters. As a consequence, the model always conveniently represents the experimental data of Table 1.

5. Results and discussion

As explained in Section 4.1, the number of Si–O–Si or Si–OH sites before deposition was fixed at 3.9×10^{14}/cm^2, corresponding to 6.5×10^{-9} kmol/m^2. This initial value appears in Fig. 4, which plots the various site numbers versus time for the experiments detailed in Table 1.

As expected, the number of Si–O–Si or Si–OH sites decreased with time, whereas that of fresh Si sites increased. The slope of all these curves logically increases with the deposition rate: the highest values are obtained for the highest deposition rates tested

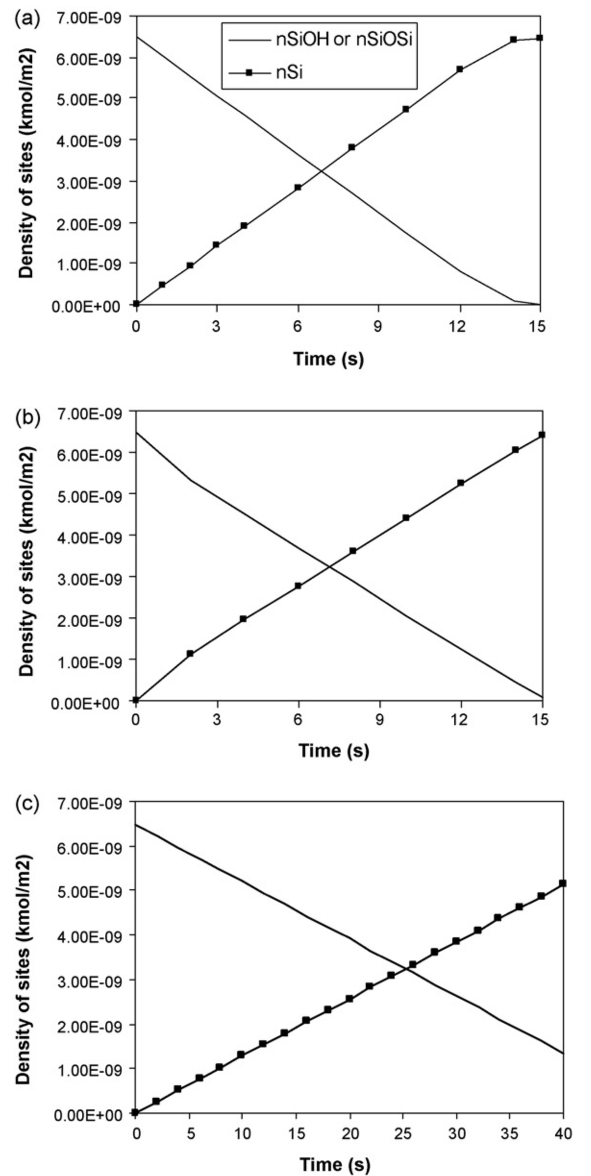

Fig. 4. Temporal evolution of the density of sites (in kmol/m^2) for runs (a) T06 and T07, (b) T31, T32 and T33 and (c) T39 and T40.

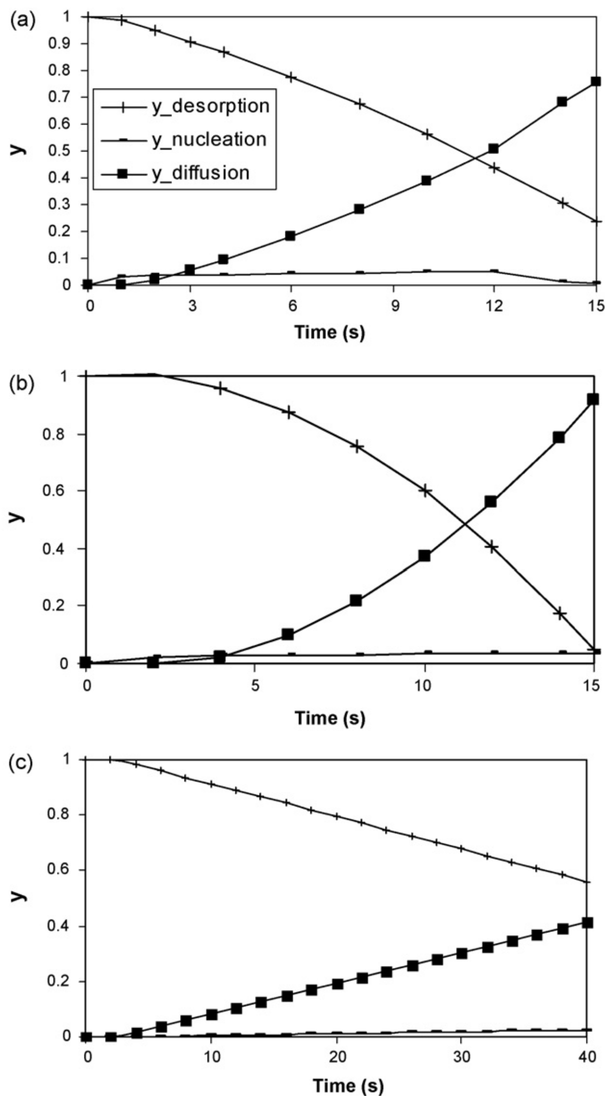

Fig. 5. Temporal evolution of the Si atom fractions from silane contributing to nucleation, surface diffusion/chemisorption and desorption for runs (a) T06 and T07, (b) T31, T32 and T33 and (c) T39 and T40.

(T06–T07 and T31–T32–T33) whereas the lowest ones correspond to runs T39–T40 (performed at the lowest pressure tested and 873 K). However, in all cases, the decrease of the Si–OH or Si–O–Si site number is rapid resulting in high proportion of substrate sites covered: the lowest value was 79% (for run T39–T40) and the highest 99% (for run T06–T07).

These quantative results must be considered with caution since as explained in Section 4.1, the number of sites on SiO_2 has probably been under-estimated.

The changes occurring with time of the fractions of Si atoms from silane contributing to nucleation, surface diffusion/chemisorption and desorption respectively are presented in Fig. 5.

First, in all cases, the mean contribution of silane to nucleation is low, less than 3% for the "non-treated" substrates and less than 3.5% for the "treated" ones. This means that the contribution to deposition of silylene on the initial substrate sites is sufficient to account for nucleation. This is a major result: our initial assumption concerning the respective roles of silane and silylene for nucleation and growth is validated.

It also appears that on "treated" substrates (T06–T07), this silane contribution to nucleation is higher than on "non-treated" substrates. The difference between the two kinds of deposition sites is due to the higher values of the experimental nucleation rate on Si–OH.

This contribution always slightly increases with time for all runs except for run T06–T07 for which it decreases for the last 3 s, because for these conditions, the whole substrate sites are covered. For the other conditions, it slightly increases with time because the deposition rate from silylene on the substrate sites always decreases with time, as detailed below.

Another major result is that between 60% and 78% in average of the silane physisorbed on the initial substrate sites must desorb to satisfy the experimental mass balance. The values are very high. As previously mentioned, they can be explained by the fact that the reactivity of the substrate sites is not high enough to enable silane to chemisorb with the same intensity as on a film composed of fresh silicon bonds. We thus quantify here the error generated by the classical law of Wilke et al. [29] for the early stages of Si deposits.

It can be further observed from Fig. 5 that the higher the deposition rate, the lower the mean desorbing fraction of silane. This trend seems to be logical since the higher the deposition rate (or the flux density of species impinging on the substrate), the greater the number of Si sites formed on the substrate and the higher the silane reactivity. The desorbing fraction logically decreases with the deposition time since the surface becomes more and more reactive toward silane.

Finally, the fraction of physisorbed silane diffusing on the surface and chemisorbing on a fresh Si site varies between 20% and 37%. It increases with run duration since the probability of chemisorption on these more and more numerous fresh Si sites increases.

At the end of the run, it exceeds 90% for run T33, meaning that the validity of the kinetic law of Wilke et al. is close to be recovered for these conditions, after 15 s of deposition. The corresponding value of the SiH_4 contribution to desorption is logically close to zero. The results are different for the two other runs: the fraction of physisorbed silane diffusing on the surface and chemisorbing on a fresh Si site at the end of run T06–T07 is equal to 75% and to 41% at the end of run T39–T40. The corresponding values of the SiH_4 contribution to desorption are respectively 24% and 56%. At the end of these experiments, Wilke et al. kinetic law is then far to be valid.

Fig. 6 gives the deposition rates versus time for the various species and types of site considered. First, it appears that for all the conditions tested whatever the type of substrate, the silylene contribution to deposition was clearly lower than that of silane, by at least two decades. This is a classical result for these LPCVD conditions, silylene being much less concentrated than silane near wafers [24].

As a consequence, and since the silane contribution to nucleation is low, the main part of the deposition comes from silane on fresh Si sites, i.e. from growth. Nucleation then appears as a mandatory step to create the first Si bonds which will then allow the main part of the deposition to occur via growth phenomena.

Consequently, the total deposition rate roughly corresponds to the silane contribution to growth. The classical influence of temperature and pressure in terms of total deposition rate and species contribution to deposition can be observed: an increase of pressure and/or of temperature leads to an increase of the total deposition rate and of the silylene contribution to deposition.

Then, it appears that in all cases the deposition rates from silane and from silylene on fresh Si sites increase with time. This result seems logical since as indicated in Table 3, the deposition rates are balanced by the number of Si sites and more and more Si sites appear with time. On Si–O–Si and Si–OH sites, the deposition rate from silylene tends to decrease since the number of substrate sites

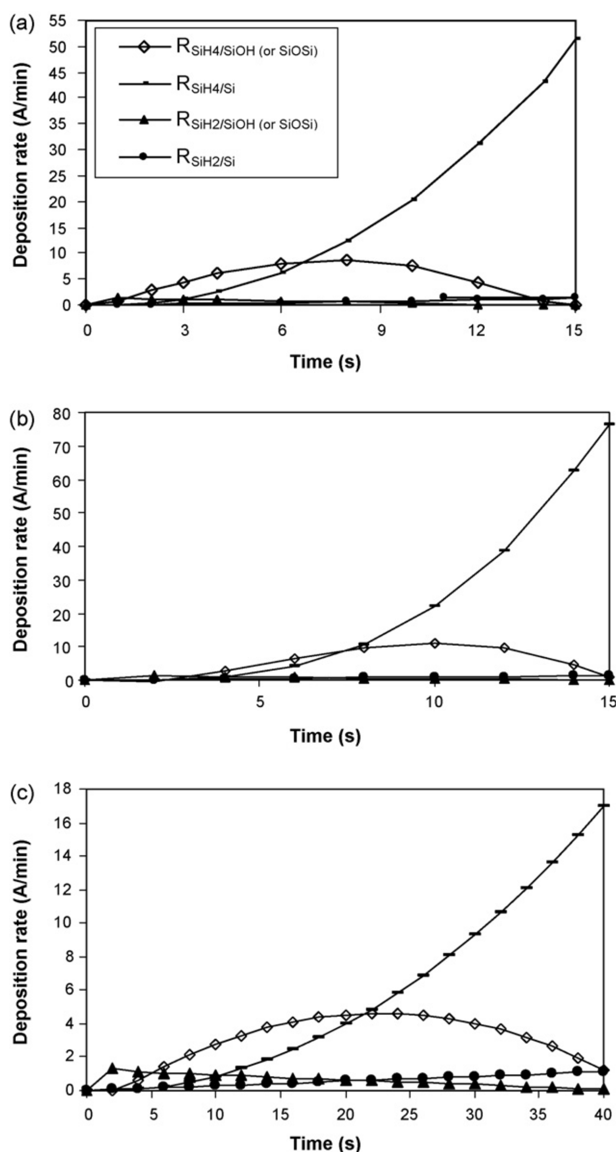

Fig. 6. Temporal evolution of the deposition rates from the various gaseous precursors (SiH_4 and SiH_2) on the different types of sites considered (SiOH or SiOSi and Si), for runs (a) T06 and T07, (b) T31, T32 and T33, (c) T39 and T40.

decreases with time. The evolution versus time of the deposition rate from silane on the SiO_2 sites is more complex: it tends first to increase then it decreases with run duration. This is due to the fact that the SiH_4 contribution to nucleation increases with time and concomitantly the number of substrate sites decreases.

Finally, another main result brought by the study is the prediction of the temporal evolution of these various deposition rates, and then of the total deposition rate, during the early stages of silicon film formation. According to Fig. 6, in all cases, the total deposition rate increases exponentially with time. This can be explained by the exponential increase of the SiH_4 reactivity of fresh Si sites. It is likely that the total deposition rate would stabilize to its maximum value a few times after the end of the runs considered, especially for run T33.

As previously explained, except for run T31–T32–T33, it always remains low in comparison with the deposition rate of classical thick Si layers. Indeed, for the conditions tested, the classical law of Wilke et al. [29] over-estimates in average by more than 60% experimental deposition rates. Such a large difference demonstrates the necessity to develop a new kinetic model valid from the early stages of deposition and accounting for the evolution with time of the nature of the substrate sites and of their reactivity.

6. Conclusion

Using the CFD code Fluent, a simulation model of an industrial hot wall LPCVD reactor has been developed for the synthesis of silicon nanodots from silane SiH_4. A comparison between experimental and calculated deposition rates has shown that classical kinetic laws largely over-estimate deposition for these ultrathin layers. The reason is that the kinetic data are valid only for continuous silicon films of conventional thickness, i.e. at least several tens of nanometers thick. During the first stage of deposition, the surface bonds present on the SiO_2 substrate play a key role and nucleation and growth phenomena are slower than on an ever growing silicon layer.

As a consequence, an original heterogeneous kinetic model has been built as a first attempt to quantify the temporal evolution of the deposition rate of each silicon precursor and of the site numbers, as a function of the operating conditions and of the chemical nature of the substrate sites. It has been assumed that the conventional law of Wilke et al. (1986) only predicts silane physisorption and that events such as silane desorption and silane chemisorption on a fresh Si site after surface diffusion are then possible. Silane and the homogeneously born silylene SiH_2 contributions to nucleation and growth have been considered on three different surface sites, silanol Si–OH, siloxane Si–O–Si and fresh Si bonds. The main mechanistic information available in the literature has been integrated in the model.

Among the main results obtained, the assumption that only silylene, and more largely all the homogeneously formed unsaturated species, contribute to nucleation has been validated for the conditions tested. The main part of deposition is due to silane via growth phenomena, i.e. on fresh Si bonds. Nucleation then appears as a mandatory step to allow the main part of deposition to occur. The deposition rate exponentially increases with time during the early stages of deposition. The classical law of Wilke et al. [29] over-estimates by between 60% and 78% in average, silicon deposition from silane during these early steps. All these results demonstrate the necessity to develop a new kinetic model valid from the early stages of Si deposition and accounting for the chemical nature of the surface sites.

Most of the results obtained can be useful for people doing CVD synthesis of nanodots. First, only silylene, and more largely all the homogeneously formed unsaturated species, contribute to nucleation. It implies that the density of nanodots could be increased either (i) by finding operating conditions (i.e. pressure, silane partial pressure,...) that would exalt silylene contribution to deposition, or (ii) by enhancing silane's ability to nucleate via new substrate pre-treatments, or (iii) by using a silicon precursor for which unsaturated species play a major role in Si deposition (like disilane). Another result concerns the fact that the main part of Si deposition results from nanodots growth (i.e. silicon deposition on already deposited silicon atoms), and is due to silane itself. So, in order to narrow the final size distribution of nanodots, a two step process of nanodots synthesis could be imagined using silane as silicon precursor: operating conditions favouring silylene contribution to deposition could be first imposed, to form a maximum of seeds and in a second part of the run, the operating parameters could be changed, (in particular, the total pressure could be decreased), to limit silylene contribution to deposition and exalt the autocatalytic contribution of silane to growth. New ways of progress are then opened.

Acknowledgment

This work has been carried out in the framework of CEA/LETI/CPMA collaboration with PLATO organization teams and tools.

References

[1] K. Makihara, H. Deki, H. Murakami, S. Higashi, S. Miyazaki, Control of the nucleation density of Si quantum dots by remote hydrogen plasma treatment, Appl. Surf. Sci. 244 (2005) 75–78.
[2] R.A. Puglisi, S. Lombardo, D. Corso, I. Crupi, G. Nicotra, L. Perniola, B. de Salvo, C. Gerardi, Effects of partial self-ordering of Si dots formed by chemical vapor deposition on the threshold voltage window distribution of Si nanocrystal memories, J. Appl. Phys. 100 (2006) 086104.
[3] F. Mazen, T. Baron, G. Brémond, J.M. Hartmann, M.N. Séméria, Influence of carrier and doping gases on the chemical vapor deposition of silicon quantum dots, Mater. Sci. Eng. B 101 (2003) 164–168.
[4] T.Z. Lu, Si nanocrystals based memories: effect of the nanocrystal density, J. Appl. Phys. 100 (2006) 014310.
[5] R.F. Steimle, R. Muralidhar, R. Rao, M. Sadd, C.T. Swift, J. Yater, B. Hradsky, S. Straub, H. Gasquet, L. Vishnubhotla, E.J. Prinz, T. Merchant, B. Acred, K. Chang, B.E. White Jr., Silicon nanocrystal non-volatile memory for embedded memory scaling, Microelectron. Reliab. 47 (2007) 585–592.
[6] G. Nicotra, S. Lomabardo, C. Spinella, G. Ammendola, C. Gerardi, C. Demuro, Observation of the nucleation kinetics of Si quantum dots on SiO_2 by energy filtered transmission electron microscopy, Appl. Surf. Sci. 205 (2003) 304–308.
[7] F. Mazen, T. Baron, G. Brémond, N. Buffet, N. Rochat, P. Mur, M.N. Séméria, Influence of the chemical properties of the substrate on silicon quantum dot nucleation, J. Electrochem. Soc. 150 (2003) G203–G208.
[8] G. Nicotra, R.A. Puglisi, S. Lombardo, C. Spinella, M. Vulpio, G. Ammendola, M. Bileci, C. Gerardi, Nucleation kinetics of Si quantum dots on SiO_2, J. Appl. Phys. 95 (2004) 2049–2055.
[9] W.T. Leach, J. Zhu, J.G. Ekerdt, Thermal desorption effects in chemical vapor deposition of silicon nanoparticles, J. Cryst. Growth 243 (2002) 30–40.
[10] J. Bloem, Nucleation and growth of silicon by CVD, J. Cryst. Growth 50 (1980) 581–604.
[11] E.F. Vansant, P. Van der Voort, K.C. Vrancken, Characterization and chemical modification of the silica surface, Studies in Surface Science and Catalysis, vol. 93, Elsevier, Amsterdam, The Netherlands, 1997.
[12] S. Miyazaki, Y. Hamamoto, E. Yoshida, M. Ikeda, M. Hirose, Control of self-assembling formation of nanometer silicon dots by low pressure chemical vapor deposition, Thin Solid Films 369 (2000) 55–59.
[13] F. Mazen, Etude de la nucléation et de la croissance de nanocristaux de silicium élaborés par dépôt chimique en phase vapeur pour dispositifs nanoélectroniques, Ph.D. Thesis INSA, Lyon, France, 2003.
[14] R.A. Puglisi, G. Nicotra, S. Lombardo, C. Spinella, G. Ammendola, M. Bileci, C. Gerardi, Exclusion zone surrounding silicon nanoclusters formed by rapid thermal chemical vapour deposition on SiO_2, Surf. Sci. 550 (2004) 119–126.
[15] Y. Kajikawa, S. Noda, Growth mode during initial stage of chemical vapor deposition, Appl. Surf. Sci. 245 (2004) 281–289.
[16] M.E. Coltrin, R.J. Kee, G.H. Evans, A mathematical model of fluid mechanics and gas-phase chemistry in a rotating disk chemical vapour deposition, J. Electrochem. Soc. 136 (1989) 819–829.
[17] P. Ho, M.E. Coltrin, W.G. Breiland, Laser-induced fluorescence measurements and kinetic analysis of Si atom formation in a rotating disk chemical vapor deposition reactor, J. Phys. Chem. 98 (1994) 10138–10147.
[18] C.R. Kleijn, A mathematical model of the hydrodynamics and gas-phase reactions in a single-wafer reactor, J. Electrochem. Soc. 138 (1991) 2190–2200.
[19] Y.B. Wang, F. Teyssandier, J. Simon, R. Feurer, Chemical vapour deposition of silicon from disilane under reduced pressure in a circular impinging jet reactor, J. Electrochem. Soc. 141 (1994) 824–843.
[20] C. Cordier, E. Dehan, E. Scheid, P. Duverneuil, Semi-insulating properties control by CVD process modelling, Mat. Sci. Eng. B 37 (1996) 30–34.
[21] C.R. Kleijn, Computational modelling of transport phenomena and detailed chemistry in chemical vapour deposition—a benchmark solution, Thin Solid Films 365 (2001) 294–306.
[22] A.M. Rinaldi, S. Carrà, M. Rampoldi, M.C. Martignoni, M. Masi, LPCVD vertical furnace optimization for undoped polysilicon film deposition, J. Phys. IV – Proc Pr8 (1999) 189–196.
[23] D. Cai, L.L. Zheng, Y. Wan, A.V. Hariharan, M. Chandra, Numerical and experimental study of polysilicon deposition on silicon tubes, J. Crys. Growth 250 (2003) 41–49.
[24] V. Cocheteau, Synthèse de plots quantiques de silicium par LPCVD pour les nouvelles générations de mémoires non volatiles, Ph.D. Thesis INP, Toulouse, France, 2005.
[25] V. Cocheteau, B. Caussat, P. Mur, E. Scheid, P. Donnadieu, T. Billon, LPCVD synthesis of silicon nanodots from silane and for flash memory devices, Electrochem. Soc. Proc. Ser. PV2005-09 (2005) 523–530.
[26] B. De Salvo, C. Gerardi, S. Lombardo, T. Baron, L. Perniola, D. Mariolle, P. Mur, A. Toffoli, M. Gely, M.N. Semeria, S. Deleonibus, G. Ammendola, V. Ancarani, M. Melanotte, R. Bez, L. Baldi, D. Corso, I. Crupi, R. A. Puglisi, G. Nicotra, E. Rimini, F. Mazen, G. Ghibaudo, G. Pananakakis, C. Monzio Compagnoni, D. Ielmini, A. Lacaita, A. Spinelli, Y. M. Wan, K. van der Jeug, How far will Silicon nanocrystals push the scaling limits of NVMs technologies, International Electron Device Meeting, Washington, December 7–10, 2003, 0-7803-7873-3/03/$17.00 © 2003 IEEE.
[27] Fluent, User Manual Fluent 6.2., 2007, http://www.Fluent.com.
[28] F. Fayolle, J.P. Couderc, P. Duverneuil, Analysis and modeling of SIPOS deposition in a hot wall tubular reactor. Part I: review of previous work and experimental study, Chem. Vap. Deposition 2 (1996) 255–263.
[29] T.E. Wilke, K.A. Turner, C.G. Takoudis, Chemical vapor deposition of silicon under reduced pressure in hot wall reactors, Chem. Eng. Sci. 41 (1986) 643–650.
[30] M. Hane, Y. Miyamoto, A. Oshiyama, Atomic and electronic structures of an interface between silicon and β-cristobalite, The American Physical Society, Phys. Rev. B 41–18 (1998) 12637–12640.